Comparative simulations of aquaporin family: AQP1, AQPZ, AQP0 and GlpF

Masanori Hashido, Mitsunori Ikeguchi, Akinori Kidera*

International Graduate School of Arts and Sciences, Yokohama City University, 1-7-29 Suehirocho, Tsurumi-ku, Yokohama 230-0045, Japan

Received 29 June 2005; revised 1 September 2005; accepted 8 September 2005

Available online 28 September 2005

Edited by Christian Griesinger

Abstract Molecular dynamics simulations were performed for four members of the aquaporin family (AQP1, AQPZ, AQP0, and GlpF) in the explicit membrane environment. The single-channel water permeability, p_f, was evaluated to be GlpF ∼ AQPZ > AQP1 ≫ AQP0, while their relative pore sizes were GlpF ≫ AQP1 > AQPZ ≫ AQP0. This relation between p_f and pore size indicates that water permeability was determined not only by the channel radius, but also another competing factor. Analysis of water dynamics revealed that this factor was the single-file nature of water transport.

Keywords: Molecular dynamics; Comparative simulation; Aquaporins; Water permeability

1. Introduction

Aquaporins (AQPs) form a large protein family of membrane channels that selectively transport water (aquaporins) or water plus glycerol (aquaglyceroporins) [1]. In studies of AQPs, molecular dynamics (MD) simulations have promoted the elucidation of the mechanisms of water permeation [2–6] and of glycerol permeation [7–9], as well as the inhibition of proton transduction [3–5,10–12].

In this study, four series of MD simulations were conducted for four members of the AQP family, AQP1 (PDB ID: 1J4N) [13], AQPZ (1RC2) [14], AQP0 (1YMG) [15], and GlpF (1LDI which does not contain glycerol in the channel) [4], in the explicit membrane environment. Each series consists of two MD trajectories of 5 ns simulations for an AQP tetramer. These AQPs have a sequence identity ranging from 28% to 49%, which increases up to 45–55% in the channel region. Their three-dimensional structures are very similar to each other; the root-mean-square displacements (RMSD) for Cα atoms are 1.7–2.3 Å for the whole chain, and 0.7–1.3 Å for the membrane spanning helices.

Comparative simulation of homologous proteins gives two advantages over the simulation of a single protein [7,16]. First, simulations under identical conditions (force field, number of water and lipid molecules, etc.) eliminate the systematic errors in the trajectories to enable quantitative comparison. Second, differences in water permeation behavior among homologous proteins are attributable to subtle variations in the amino acids and structures in the channel region. Here, we exploited these advantages of comparative simulation to determine the relation between channel structure and water permeation rate in AQPs at atomic resolution.

2. Materials and methods

2.1. Molecular dynamics simulations

The tetrameric form of aquaporin (AQP1:1J4N, AQPZ:1RC2, or AQP0:1YMG) or aquaglyceroporin (GlpF:1LDI) was embedded in a equilibrated palmitoyl-oleoyl-phosphatidyl-choline (POPC) lipid bilayer. After removal of the lipid molecules that overlapped with the protein, the positions and orientations of the surrounding lipid molecules were optimized. The system contains about 390 lipid molecules and 30 000 waters. This embedding process was repeated for each of 5 ns simulations to produce a different membrane environment in each run. Each system was equilibrated for 400 ps with constraining the coordinates of the protein under the NPT condition (300.15 K and 1 atm). Then, after gradually releasing the constraints over 100 ps, the product run was performed under the NPT condition for 5 ns without any additional constraint. The equilibration and product runs were performed twice for each of four proteins; the total simulation time of product runs was 40 ns (5 ns × 2 run × 4 proteins). All simulations were performed using MARBLE [17] with CHARMM 22 force field [18] corrected by CMAP [19] for proteins, CHARMM 27 [20] for lipids, and TIP3P for water [21]. Electrostatic calculations were performed using the Particle Mesh Ewald method with the periodic boundary conditions [22]. To make all systems electrically neutral, suitable numbers of counter ions were added to the bulk water. The Lennard-Jones interactions were switched to zero over a range of 8–10 Å. The symplectic integrator for rigid bodies was used with a time step of 2 fs, in which water and CH_x, NH_x (x = 1, 2, or 3), SH, and OH groups were treated as rigid bodies [17]. The entire system, an AQP tetramer, lipid molecules, waters, and counter ions, contains about 150 000 atoms.

2.2. Channel radius

To calculate the channel radius, a program based on the method of Smart et al. [23] was used. The algorithm uses a Monte Carlo simulated annealing to find a suitable radius for a sphere probe, which moves on the x–y plane to search for vacant areas. For the calculations, atomic radii were set to values yielding zero for the radial distribution function.

2.3. Water–water correlation

To analyze correlation in motion between neighboring water molecules inside the channel, we used the following correlation function, $c(z)$:

$$c(z) = \frac{\langle \delta z_i \delta z_j \rangle}{(\langle \delta z_i^2 \rangle \langle \delta z_j^2 \rangle)^{1/2}}, \quad (1)$$

*Corresponding author. Fax: +81 45 508 7367.
E-mail addresses: hashido@tsurumi.yokohama-cu.ac.jp (M. Hashido), ike@tsurumi.yokohama-cu.ac.jp (M. Ikeguchi), kidera@tsurumi.yokohama-cu.ac.jp (A. Kidera).

0014-5793/$30.00 © 2005 Published by Elsevier B.V. on behalf of the Federation of European Biochemical Societies.
doi:10.1016/j.febslet.2005.09.018

where z is the average position of the two neighboring water molecules i and j in the channel. The distance between the two water molecules is less than 3.5 Å, and δz_i is defined by,

$$\delta z_i = z_i(t) - z_i(t + \Delta t), \quad (2)$$

where $z_i(t)$ is the coordinate of water i at t. Here, we set $\Delta t = 30$ ps.

3. Results and discussion

Water permeation through the AQP channel was almost perfectly diffusive as shown in Fig. 1a; the mean square displacement of water molecules along the channel was proportional to time except for the short time scale. Below 10 ps, water exhibited jumping motions between the preferential sites (see Fig. 2c for details), resulting in slightly larger slopes in this time range. The single-channel water permeability, p_f, was evaluated from the diffusion coefficients (the slopes of Fig. 1a) by the method of Zhu et al. [24], and summarized in Fig. 1b.

Reported experimental values of p_f (at 10^{-14} cm^3/s) are 4.6 [25], 5.43 [26], 6 [27], and 11.7 [28] for AQP1, $\geqslant 10$ for AQPZ [29], 0.25 for AQP0 [27], and about 2 (estimated from membrane permeability) for GlpF [30]. Reported values of p_f derived from MD simulations are 7.1 for AQP1 [31] and 14 for GlpF [6]. These experimental and simulation data agree well with the results presented in Fig. 1b, except for the experimental value for GlpF, which is nearly one order of magnitude smaller than both the value of the present simulation and that of Zhu et al. [6]. Considering the good agreement between the two simulation results for GlpF, it is likely that the simulations for GlpF possess an intrinsic problem that causes the discrepancies from the experimental results. It should be remarked, however, that the comparison of p_f values between experiments and simulations has to be done with great care because experimental p_f values tend to have large errors depending on the accuracy of estimated number of channels in the sample.

3.1. Comparison between AQP1 and AQPZ

The values of p_f for AQP1 and AQPZ were calculated as 10 ± 4 and 16 ± 5, respectively (Fig. 1b). Here, we consider the structural basis of the 60% difference in water permeation.

Eight atoms hydrogen bonded with the channel waters primarily determine the channel shape and the peak positions of water density as shown in Fig. 2c (Fig. 2 contains the atom list). The RMSD for the eight atoms between AQP1 and AQPZ was calculated as small as 0.3 Å. This similarity is reflected in the similar profiles of channel radius shown in Fig. 2b. However, in the NPA region, the change from Val178 of AQP1 to Leu170 of AQPZ (Fig. 2f) diminishes the channel radius by 0.35 Å, as depicted in Fig. 2a. As a result, AQPZ allows just one water molecule to occupy the NPA region, while AQP1 can accept two water molecules there; the number of water molecules in the NPA region calculated by integrating water density in Fig. 2c is 1.23 for AQP1 and 0.90 for AQPZ. This difference directly influences the correlation in motion between two neighboring water molecules (Fig. 2d); correlation in AQPZ is larger by 0.08 than that of AQP1. If there is room for two water molecules in the NPA region as in AQP1, the motion of a water molecule is not effectively propagated to neighboring waters, but is transferred to the vacant site. On the other hand, AQPZ has more single file like permeation, or a less compressible water file to yield a larger value of p_f.

3.2. Small but nonzero p_f value in AQP0

The extremely small value of p_f in AQP0, 0.2 ± 0.2, is attributable to two Tyr residues, Tyr23 in the NPA region and Tyr149 at about −16 Å (Fig. 2f). These Tyr residues plug the channel to reduce channel radius (Fig. 2b) and restrain the water flow to produce high and sharp water density exclusively at the preferential sites (Fig. 2c). However, the p_f value is not zero. We observed seven times water permeation through the NPA region during two of the 5 ns simulations. One permeation event is illustrated in Fig. 3. First, water forms a hydrogen bond with the OH group of Tyr, followed by a flipping motion of Tyr that appears to protrude the water.

It is of interest to observe the similar orientation of water dipoles in AQP0 as in the other AQPs. As shown in previous simulations [4] and in Fig. 2e, water dipole reverses direction when passing across the NPA region. This is one of the mechanisms of preventing proton transduction. It has been argued that the orientation of water dipoles is controlled by hydrogen bonding with the NPA motifs and the macro-dipoles formed by the hemi-helices (helix HB and HE) [4]. However, since AQP0 prohibits hydrogen bond formation between the NPA motifs and water, the macro-dipoles must be the exclusive determinant of water orientation.

3.3. Comparison between AQPZ and GlpF

AQPZ and GlpF have similar values of p_f, 16 ± 5 and 16 ± 3, respectively, although the channel radius is much larger in

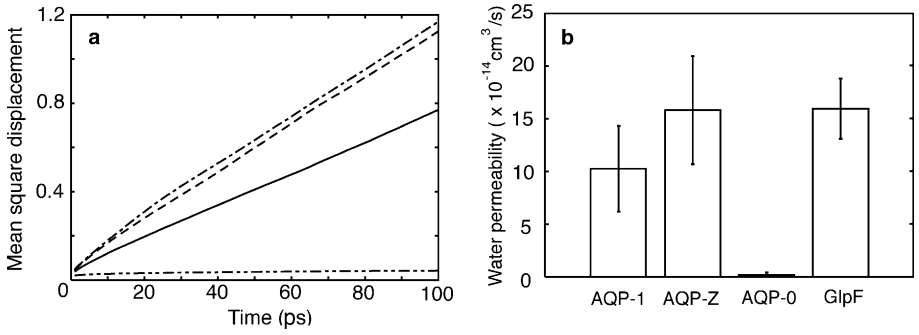

Fig. 1. (a) Linear time dependence of mean square displacements of the collective coordinates defined by $dn = \sum_{i \in C(t)} dz_i / L$, where dz_i is the displacement of water i, $C(t)$ denotes the water molecules in the channel at time t, and L is the channel length (=16 Å, $-13 < z < 3$) evaluated from the water density distribution (Fig. 2c). The dash-dotted line, dashed line, solid line, and dash-double dotted line represent GlpF, AQPZ, AQP1, and AQP0, respectively. (b) Single-channel water permeability, p_f. Error bars indicate the S.D. from eight trajectories of each channel.

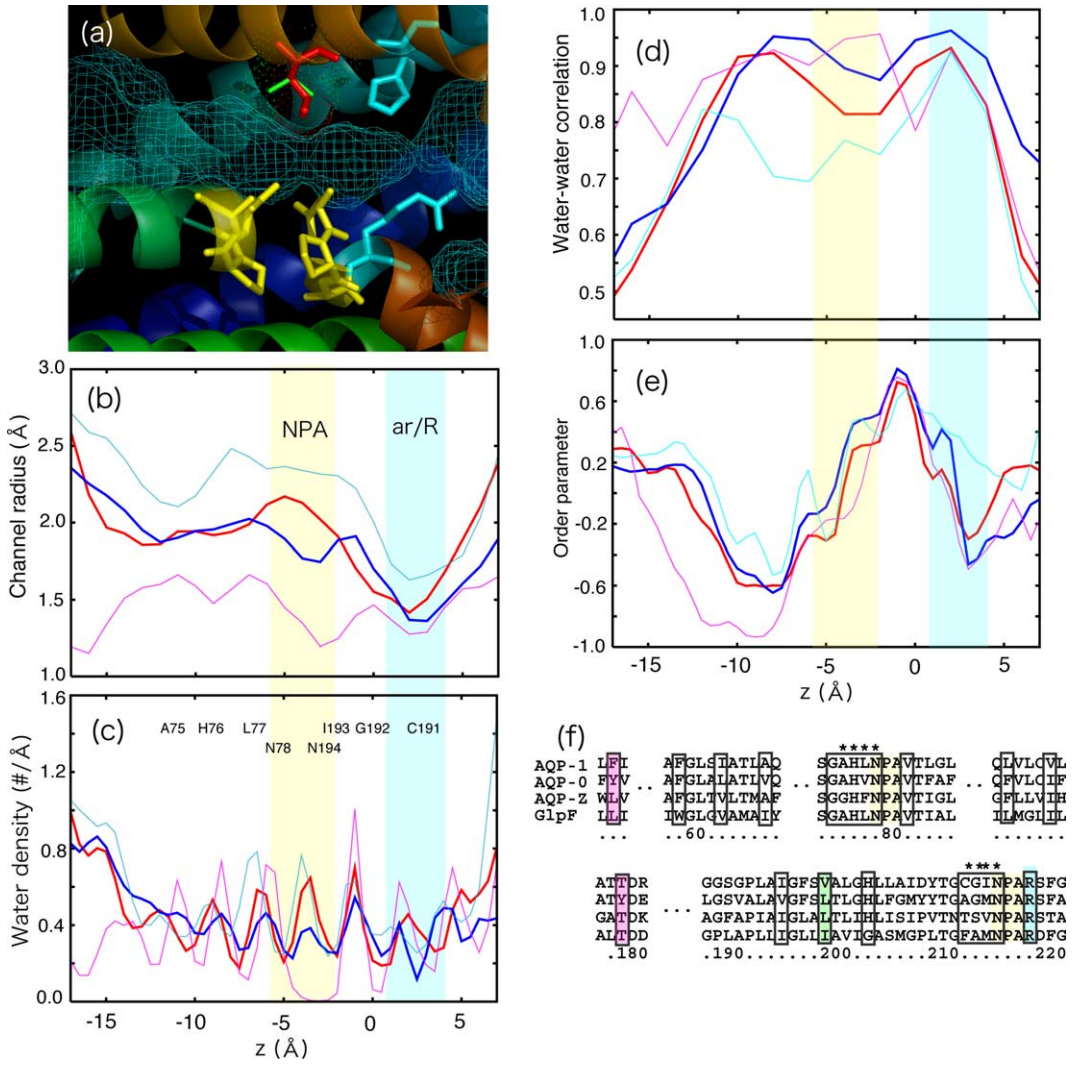

Fig. 2. (a) The channel region of an AQP monomer based on the AQP1 coordinates. Residues lining the pore are shown in the stick model; the NPA motifs (yellow), the ar/R region (cyan), and Val178 of AQP1 (green). Leu170 of AQPZ (red) was superimposed on Val178 of AQP1. The channel surface of AQPZ, indicated by light-blue mesh, shows a concave shape at Leu170. The z-direction was defined by the membrane normal. The z-coordinates were superimposed by setting O of G192 of AQP1 to $z = 0$. This figure was prepared with Pymol (www.pymol.org)[32]. (b) Effective channel radius of the AQPs calculated by the average of eight trajectories of 5 ns simulations: AQP1 (red), AQPZ (blue), AQP0 (magenta) and GlpF (cyan). The NPA and ar/R regions are indicated by transparent yellow and cyan, respectively. (c) Distribution of water density inside the channel. Bin size is 0.5 Å. The peak positions of water density contain the hydrogen bond partners of water molecules: (left to right) O of A75, O of H76, O of I77, Nδ of N78, Nδ of N194, O of 193I, O of 192G, and O of 191C (the sequence is after AQP1). (d) Correlation in motions between neighboring water molecules inside the channel as calculated by Eq. (1). (e) Orientation of water molecules in the channel, calculated as the order parameter, $P_1(z) = \langle \cos\theta \rangle$, where θ is the angle between the membrane normal and the water dipole vector. (f) Multiple sequence alignment of aquaporins and aquaglyceroporins. Channel forming residues are enclosed by frames. The NPA motifs and ar/R region are yellow and cyan, respectively. Green residues correspond to Val178 of AQP1 and Leu170 of AQPZ shown in Fig. 1(a). Magenta residues correspond to Tyr23 and Tyr149 of AQP0. Asterisks indicate the residues hydrogen bonded with water molecules. The other residues contribute to the channel surface via side-chains.

GlpF than in AQPZ. As discussed above, the efficiency of water permeation is determined not only by channel width but also the single-file nature or a less compressible structure of the water file. The latter determines the difference in permeability between AQP1 and AQPZ. Fig. 2d shows very small values of water–water correlation in GlpF, indicating that GlpF has a highly compressible water file; the number of water molecules in the NPA region is 1.3. The large channel width may compensate for the reduction of the permeation rate due to the highly compressible structure of the water file, and eventually yield a value of p_f similar to that of AQPZ. Considering the channel size of GlpF, it may be difficult for a simulation to give the small experimental value of p_f (about 2). Therefore, it is reasonable to suppose a factor reducing channel size under the experimental condition.

In summary, water permeability was determined not only by channel radius, but also the single-file character of water transportation. This single-file character diminishes with increasing channel size; thus permeation rate does not increase with the pore size. On the other hand, when the channel is too narrow to form a single file of water molecules, the permeation rate becomes small like in AQP0. Results indicated that the order of the permeation rate was GlpF $\sim$ AQPZ > AQP1 $\gg$ AQP0, while the relative pore size was GlpF $\gg$ AQP1 > AQPZ $\gg$ AQP0.

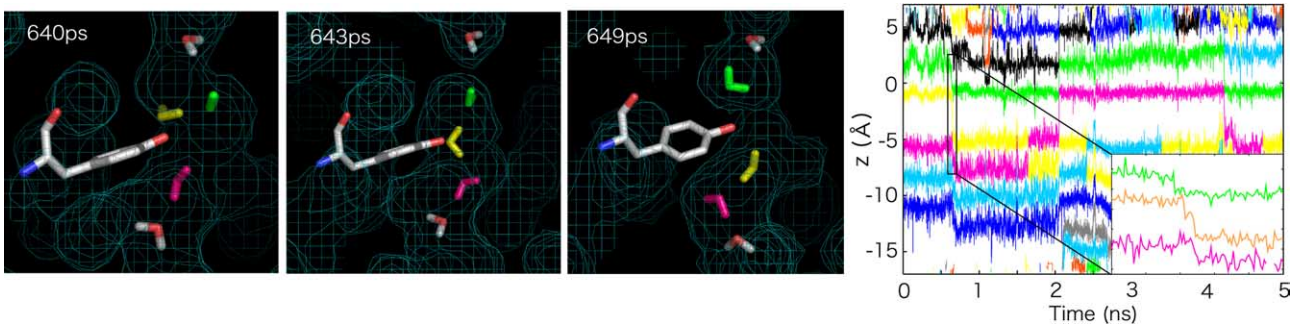

Fig. 3. Snapshots of a water permeation process across the NPA region of AQP0. Tyr23 is illustrated by a stick model. Water molecules are yellow, green and pink. The right plot indicates trajectories of water in the channel. Colors of lines in the expanded plot correspond to those of the water in the snapshots.

Acknowledgments: The authors thank Drs. K. Mitsuoka and Y. Fujiyoshi for valuable discussion. This study was supported by a Grant-in-Aid for Scientific Research on Priority Areas (membrane interface) from the Ministry of Education, Science and Culture of Japan.

References

[1] Borgnia, M., Nielsen, S., Engel, A. and Agre, P. (1999) Cellular and molecular biology of the aquaporin water channels. Annu. Rev. Biochem. 68, 425–458.
[2] Zhu, F., Tajkhorshid, E. and Schulten, K. (2001) Molecular dynamics study of aquaporin-1 water channel in a lipid bilayer. FEBS Lett. 504, 212–218.
[3] de Groot, B.L. and Grubmüller, H. (2001) Water permeation across biological membrane: mechanism and dynamics of aquaporin-1 and GlpF. Science 294, 2353–2357.
[4] Tajkhorshid, E., Nollert, P., Jensen, M.Ø., Miercke, L.J.W., O'Connell, J., Stroud, R.M. and Schulten, K. (2002) Control of the selectivity of the aquaporin water channel family by global orientational tuning. Science 296, 525–530.
[5] Jensen, M.Ø., Tajkhorshid, E. and Schulten, K. (2003) Electrostatic tuning of permeation and selectivity in aquaporin water channels. Biophys. J. 85, 2884–2899.
[6] Zhu, F., Tajkhorshid, E. and Schulten, K. (2002) Pressure-induced water transport in membrane channels studied by molecular dynamics. Biophys. J. 83, 154–160.
[7] Wang, Y., Schulten, K. and Tajkhorshid, E. (2005) What makes an aquaporin a glycerol channel? A comparative study of AQPZ and GlpF. Structure 13, 1107–1118.
[8] Jensen, M.Ø., Tajkhorshid, E. and Schulten, K. (2001) The mechanism of glycerol conduction in aquaglyceroporins. Structure 9, 1083–1093.
[9] Jensen, M.Ø., Park, S., Tajkhorshid, E. and Schulten, K. (2002) Energetics of glycerol conduction through aquaglyceroprin GlpF. Proc. Natl. Acad. Sci. USA 99, 6731–6736.
[10] de Groot, B.L., Frigato, T., Helms, V. and Grubmüller, H. (2003) The mechanism of proton exclusion in the aquaporin-1 water channel. J. Mol. Biol. 333, 279–293.
[11] Chakrabarti, N., Tajkhorshid, E., Roux, B. and Pomes, R. (2004) Molecular basis of proton blockage in aquaporins. Structure 12, 65–74.
[12] Ilan, B., Tajkhorshid, E., Schulten, K. and Voth, G.A. (2004) The mechanism of proton exclusion in aquaporin channels. Proteins 55, 223–228.
[13] Sui, H., Han, B.G., Lee, J.K., Walian, P. and Jap, B.K. (2001) Structural basis of water-specific transport through the AQP1 water channel. Nature 414, 872–878.
[14] Savage, D.F., Egea, P.F., Robles-Colmenares, Y., O'Connell, J.D. and Stroud, R.M. (2003) Architecture and selectivity in aquaporins: 2.5 Å X-ray structure of aquaporin-Z. PLoS Biol. 1, 334–340.
[15] Harries, W.E.C., Akhavan, D., Miercke, L.J.W., Khademi, S. and Stroud, R.M. (2004) The channel architecture of aquaporin 0 at a 2.2 Å resolution. Proc. Natl. Acad. Sci. USA 101, 14045–14050.
[16] Deol, S.S., Bond, P.J., Domene, C. and Sansom, M.S.P. (2004) Lipid–protein interactions of integral membrane proteins: a comparative simulation study. Biophys. J. 87, 3737–3749.
[17] Ikeguchi, M. (2004) Partial rigid-body dynamics in NPT, NPAT and NPγT ensembles for proteins and membranes. J. Comput. Chem. 25, 529–541.
[18] MacKerell Jr., A.D., Bashford, D., Bellott, M., Dunbrack Jr., R.L., Evanseck, J.D., Field, M.J., Fischer, S., Gao, J., Guo, H., Ha, S., Joseph-McCarthy, D., Kuchnir, L., Kuczera, K., Lau, F.T.K., Mattos, C., Michnick, S., Ngo, T., Dguyen, D.T., Prodhom, B., Reiher III, W.E., Roux, B., Schlenkrich, M., Smith, J.C., Stote, R., Straub, J., Watanabe, M., Wiorkiewicz-Kuczera, J., Yin, D. and Karplus, M.J. (1998) All-atom empirical potential for molecular modeling and dynamics studies of proteins. Phys. Chem. B 102, 3586–3616.
[19] MacKerell Jr., A.D., Feig, M. and Brooks III, C.L. (2004) Empirical force fields for biological macromolecules: overview and issues. J. Comput. Chem. 25, 1400–1415.
[20] Feller, S.E. and MacKerell, A.D. (2000) An improved empirical potential energy function for molecular simulations of phospholipids. J. Phys. Chem. B 104, 7510–7515.
[21] Jorgensen, W.L., Chandrasekhar, J., Madura, J.D., Impey, R.W. and Klein, M.L. (1983) Comparison of simple potential fuctions for simulating liquid water. J. Chem. Phys. 79, 926–935.
[22] Essmann, U., Perera, L., Berkowitz, M.L., Darden, T., Lee, H. and Pedersen, L.G. (1995) A smooth particle mesh Ewald method. J. Chem. Phys. 103, 8577–8593.
[23] Smart, O.S., Goodfellow, J.M. and Wallace, B.A. (1993) The pore dimensions of Gramicidin A. Biophys. J. 65, 2455–2460.
[24] Zhu, F., Tajkhorshid, E. and Schulten, K. (2004) Collective diffusion model for water permeation through microscopic channels. Phys. Rev. Lett. 93, 224501–224505.
[25] Zeidel, M.L., Nielsen, S., Smith, B.L., Ambudkar, S.V., Maunsbach, A.B. and Agre, P. (1994) Ultrastructure, pharmacologic inhibition, and transport selectivity of aquaporin channel-forming integral protein in proteoliposomes. Biochemistry 33, 1606–1615.
[26] Walz, T., Smith, B.L., Zeidel, M.L., Engel, A. and Agre, P. (1994) Biological active two-dimensional crystals of aquaporin CHIP. J. Biol. Chem. 269, 1583–1586.
[27] Yang, B. and Verkman, A.S. (1997) Water and glycerol permeabilities of aquaporins 1–5 and MIP determined quantitatively by expression of epitope-tagged constructs in *Xenopus* Oocytes. J. Biol. Chem. 272 (26), 16140–16146.
[28] Zeidel, M.L., Ambudkar, S.V., Smith, B.L. and Agre, P. (1992) Reconstitution of functional water channels in liposomes containing purified red cell CHIP28 protein. Biochemistry 31, 7436–7440.
[29] Borgnia, M.J., Kozono, D., Calamita, G., Maloney, P.C. and Agre, P. (1999) Functional reconstitution and characterization of AQPZ, the *E. coli* water channel protein. J. Mol. Biol. 291, 1169–1179.
[30] Borgnia, M.J. and Agre, P. (2001) Reconstitution and functional comparison of purified GlpF and AQPZ, the glycerol and water channels from *Escherichia coli*. Proc. Natl. Acad. Sci. USA 98, 2888–2893.
[31] Zhu, F., Tajkhorshid, E. and Schulten, K. (2004) Theory and simulation of water permation in aquaporin-1. Biophys. J. 86, 50–57.
[32] DeLano, W.L. (2002) The PyMOL Molecular Graphics System, DeLano Scientific, San Carlos, CA, USA.